COLEÇÃO

DESAFIOS DAS ENGENHARIAS:

ENGENHARIA ELÉTRICA 2

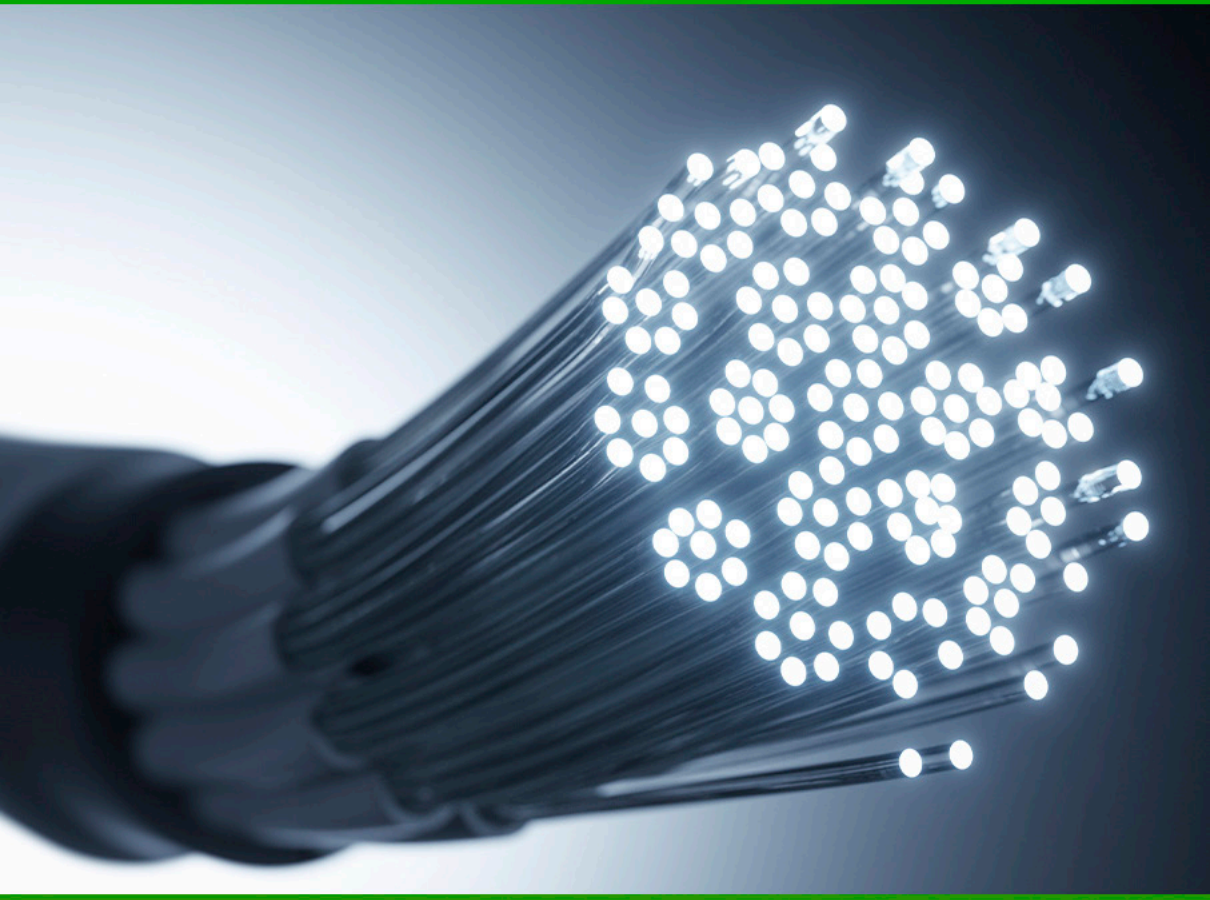

JOÃO DALLAMUTA
HENRIQUE AJUZ HOLZMANN
(ORGANIZADORES)

Atena Editora
Ano 2021

COLEÇÃO

DESAFIOS DAS ENGENHARIAS:

ENGENHARIA ELÉTRICA 2

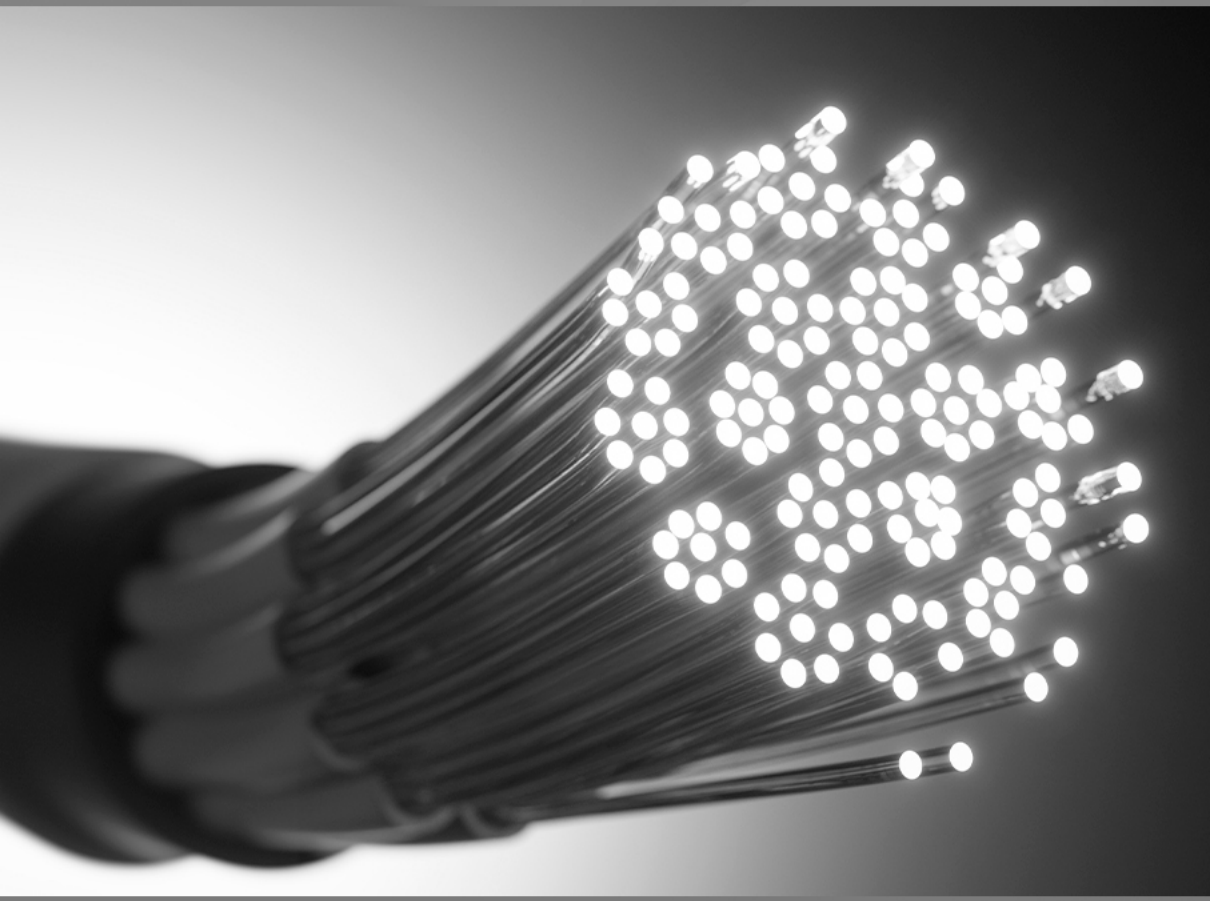

JOÃO DALLAMUTA
HENRIQUE AJUZ HOLZMANN
(ORGANIZADORES)

Atena Editora
Ano 2021

Editora chefe
Profª Drª Antonella Carvalho de Oliveira
Editora executiva
Natalia Oliveira
Assistente editorial
Flávia Roberta Barão
Bibliotecária
Janaina Ramos
Projeto gráfico
Camila Alves de Cremo
Daphynny Pamplona
Luiza Alves Batista
Maria Alice Pinheiro
Natália Sandrini de Azevedo
Imagens da capa
iStock
Edição de arte
Luiza Alves Batista

2021 *by Atena Editora*
Copyright © Atena Editora
Copyright do texto © 2021 Os autores
Copyright da edição © 2021 Atena Editora
Direitos para esta edição cedidos à Atena Editora pelos autores.
Open access publication by Atena Editora

Todo o conteúdo deste livro está licenciado sob uma Licença de Atribuição *Creative Commons*. Atribuição-Não-Comercial-NãoDerivativos 4.0 Internacional (CC BY-NC-ND 4.0).

O conteúdo dos artigos e seus dados em sua forma, correção e confiabilidade são de responsabilidade exclusiva dos autores, inclusive não representam necessariamente a posição oficial da Atena Editora. Permitido o *download* da obra e o compartilhamento desde que sejam atribuídos créditos aos autores, mas sem a possibilidade de alterá-la de nenhuma forma ou utilizá-la para fins comerciais.

Todos os manuscritos foram previamente submetidos à avaliação cega pelos pares, membros do Conselho Editorial desta Editora, tendo sido aprovados para a publicação com base em critérios de neutralidade e imparcialidade acadêmica.

A Atena Editora é comprometida em garantir a integridade editorial em todas as etapas do processo de publicação, evitando plágio, dados ou resultados fraudulentos e impedindo que interesses financeiros comprometam os padrões éticos da publicação. Situações suspeitas de má conduta científica serão investigadas sob o mais alto padrão de rigor acadêmico e ético.

Conselho Editorial
Ciências Exatas e da Terra e Engenharias
Prof. Dr. Adélio Alcino Sampaio Castro Machado – Universidade do Porto
ProFª Drª Ana Grasielle Dionísio Corrêa – Universidade Presbiteriana Mackenzie
Prof. Dr. Carlos Eduardo Sanches de Andrade – Universidade Federal de Goiás
Profª Drª Carmen Lúcia Voigt – Universidade Norte do Paraná
Prof. Dr. Cleiseano Emanuel da Silva Paniagua – Instituto Federal de Educação, Ciência e Tecnologia de Goiás

Atena Editora
Ano 2021

Prof. Dr. Douglas Gonçalves da Silva – Universidade Estadual do Sudoeste da Bahia
Prof. Dr. Eloi Rufato Junior – Universidade Tecnológica Federal do Paraná
Profª Drª Érica de Melo Azevedo – Instituto Federal do Rio de Janeiro
Prof. Dr. Fabrício Menezes Ramos – Instituto Federal do Pará
Profª Dra. Jéssica Verger Nardeli – Universidade Estadual Paulista Júlio de Mesquita Filho
Prof. Dr. Juliano Carlo Rufino de Freitas – Universidade Federal de Campina Grande
Profª Drª Luciana do Nascimento Mendes – Instituto Federal de Educação, Ciência e Tecnologia do Rio Grande do Norte
Prof. Dr. Marcelo Marques – Universidade Estadual de Maringá
Prof. Dr. Marco Aurélio Kistemann Junior – Universidade Federal de Juiz de Fora
Profª Drª Neiva Maria de Almeida – Universidade Federal da Paraíba
Profª Drª Natiéli Piovesan – Instituto Federal do Rio Grande do Norte
Profª Drª Priscila Tessmer Scaglioni – Universidade Federal de Pelotas
Prof. Dr. Sidney Gonçalo de Lima – Universidade Federal do Piauí
Prof. Dr. Takeshy Tachizawa – Faculdade de Campo Limpo Paulista

Atena Editora
Ano 2021

Ciências Exatas e da Terra e Engenharias

Coleção desafios das engenharias: engenharia elétrica 2

Diagramação: Daphynny Pamplona
Correção: Flávia Roberta Barão
Indexação: Gabriel Motomu Teshima
Revisão: Os autores
Organizadores: João Dallamuta
Henrique Ajuz Holzmann

Dados Internacionais de Catalogação na Publicação (CIP)

C691 Coleção desafios das engenharias: engenharia elétrica 2 / Organizadores João Dallamuta, Henrique Ajuz Holzmann. – Ponta Grossa - PR: Atena, 2021.

Formato: PDF
Requisitos de sistema: Adobe Acrobat Reader
Modo de acesso: World Wide Web
Inclui bibliografia
ISBN 978-65-5983-556-0
DOI: https://doi.org/10.22533/at.ed.560211910

1. Engenharia elétrica. I. Dallamuta, João (Organizador). II. Holzmann, Henrique Ajuz (Organizador). III. Título.

CDD 621.3

Elaborado por Bibliotecária Janaina Ramos – CRB-8/9166

Atena Editora
Ponta Grossa – Paraná – Brasil
Telefone: +55 (42) 3323-5493
www.atenaeditora.com.br
contato@atenaeditora.com.br

Atena Editora
Ano 2021

DECLARAÇÃO DOS AUTORES

Os autores desta obra: 1. Atestam não possuir qualquer interesse comercial que constitua um conflito de interesses em relação ao artigo científico publicado; 2. Declaram que participaram ativamente da construção dos respectivos manuscritos, preferencialmente na: a) Concepção do estudo, e/ou aquisição de dados, e/ou análise e interpretação de dados; b) Elaboração do artigo ou revisão com vistas a tornar o material intelectualmente relevante; c) Aprovação final do manuscrito para submissão.; 3. Certificam que os artigos científicos publicados estão completamente isentos de dados e/ou resultados fraudulentos; 4. Confirmam a citação e a referência correta de todos os dados e de interpretações de dados de outras pesquisas; 5. Reconhecem terem informado todas as fontes de financiamento recebidas para a consecução da pesquisa; 6. Autorizam a edição da obra, que incluem os registros de ficha catalográfica, ISBN, DOI e demais indexadores, projeto visual e criação de capa, diagramação de miolo, assim como lançamento e divulgação da mesma conforme critérios da Atena Editora.

Atena Editora
Ano 2021

DECLARAÇÃO DA EDITORA

A Atena Editora declara, para os devidos fins de direito, que: 1. A presente publicação constitui apenas transferência temporária dos direitos autorais, direito sobre a publicação, inclusive não constitui responsabilidade solidária na criação dos manuscritos publicados, nos termos previstos na Lei sobre direitos autorais (Lei 9610/98), no art. 184 do Código Penal e no art. 927 do Código Civil; 2. Autoriza e incentiva os autores a assinarem contratos com repositórios institucionais, com fins exclusivos de divulgação da obra, desde que com o devido reconhecimento de autoria e edição e sem qualquer finalidade comercial; 3. Todos os e-book são *open access, desta forma* não os comercializa em seu site, sites parceiros, plataformas de *e-commerce,* ou qualquer outro meio virtual ou físico, portanto, está isenta de repasses de direitos autorais aos autores; 4. Todos os membros do conselho editorial são doutores e vinculados a instituições de ensino superior públicas, conforme recomendação da CAPES para obtenção do Qualis livro; 5. Não cede, comercializa ou autoriza a utilização dos nomes e e-mails dos autores, bem como nenhum outro dado dos mesmos, para qualquer finalidade que não o escopo da divulgação desta obra.

Atena Editora
Ano 2021

APRESENTAÇÃO

A engenharia elétrica tornou-se uma profissão há cerca de 130 anos, com o início da distribuição de eletricidade em caráter comercial e com a difusão acelerada do telégrafo em escala global no final do século XIX.

Na primeira metade do século XX a difusão da telefonia e da radiodifusão além do crescimento vigoroso dos sistemas elétricos de produção, transmissão e distribuição de eletricidade, deu os contornos definitivos para a carreira de engenheiro eletricista que na segunda metade do século, com a difusão dos semicondutores e da computação gerou variações de ênfase de formação como engenheiros eletrônicos, de telecomunicações, de controle e automação ou de computação.

Produzir conhecimento em engenharia elétrica é portando pesquisar em uma gama enorme de áreas, subáreas e abordagens de uma engenharia que é onipresente em praticamente todos os campos da ciência e tecnologia.

Neste livro temos uma diversidade de temas, níveis de profundidade e abordagens de pesquisa, envolvendo aspectos técnicos e científicos. Aos autores e editores, agradecemos pela confiança e espirito de parceria.

João Dallamuta

Henrique Ajuz Holzmann

SUMÁRIO

CAPÍTULO 1

PHOTODETECTOR OPTIC POWER OPTIMIZATION TO INCREASE THE GAIN ON SUB-OCTAVE MICROWAVE PHOTONIC LINK

Data de aceite: 01/10/2021
Data de Submissão: 06/07/2021

Naiara Tieme Mippo
Instituto Tecnológico de Aeronáutica (ITA)
São José dos Campos – SP
http://lattes.cnpq.br/3471863952786744

Paulo Henrique Kiohara Acyoli Bastos
Instituto Tecnológico de Aeronáutica (ITA)
São José dos Campos – SP
http://lattes.cnpq.br/4315870934146368

Felipe Streitenberger Ivo
Instituto Tecnológico de Aeronáutica (ITA)
São José dos Campos – SP
http://lattes.cnpq.br/0013935085701273

Olympio Lucchini Coutinho
Instituto Tecnológico de Aeronáutica (ITA)
São José dos Campos – SP
http://lattes.cnpq.br/4324540631101004

ABSTRACT: An investigation of the optic spectral components beating at the photodetector to recover the RF signal at the output of a sub-octave microwave photonic link is presented, by a theoretical and experimental approach. It is demonstrated the best efficiency is achieved when the carrier to sideband ratio (CSR) is 0 dB at a low bias voltage condition on Mach-Zehnder (MZM) intensity modulator. A RF power link gain improvement of 9.7 dB is demonstrated for a same photodetector incident optic power, compared with a link operating at quadrature bias voltage condition on the MZM.
KEYWORDS: Fiber optic links; low bias photonic links, microwave photonics.

OPTIMIZAÇÃO DA POTÊNCIA ÓPTICA NO FOTODETECTOR PARA AUMENTO DO GANHO NO ENLACE ANALÓGICO A FIBRA ÓPTICA DE SUB-OITAVA

RESUMO: A análise do batimento entre componentes ópticas espectrais no fotodetector para recuperação do sinal RF na saída de um enlace analógico a fibra óptica de sub-oitava é apresentada através de abordagens teóricas e experimentais. Demonstra-se que a melhor eficiência é atingida quando a diferença entre amplitudes das componentes da portadora óptica e das bandas laterais é 0 dB, condição de baixa tensão de polarização no modulador de intensidade Mach-Zehnder. Uma melhora de 9,7 dB no ganho do enlace é demonstrada neste ponto de operação em comparação com o modulador Mach-Zehnder polarizado em quadratura, com mesma potência óptica incidente no fotodetector.
PALAVRAS-CHAVE: Enlace analógico a fibra óptica; enlace fotônico sob baixa polarização; RF em fotônica.

1 I INTRODUCTION

Microwave photonics (MWP) has been considered a promising technology to implement RF functionalities at high frequency and high bandwidth (BW) long distance transmission lines

and signal processing systems, where conventional electronics circuits based on coaxial cables, waveguides and printed circuits boards (PCB) face limitations, due to high propagation losses and circuitry complexities [2]. The electronic circuit behavior is strongly dependent to the wavelength, and it brings severe design limitations for high bandwidth systems, where the start frequency is far from the stop frequency. In contrast, microwave photonics principle basically consists in modulating an optical carrier with the RF signal, to transmits and processes it at the optic spectrum and finally recover it at the system output by photodetection. The RF signal modulates an optic carrier at frequencies about 200 THz, producing a very low change on the wavelength among all the system bandwidth. Besides, fiber optic also offers other advantages like electromagnetic interference immunity (EMI), low weight and size. Those characteristics have been attracted attention to modern microwave systems implementation on civilian and military application, such as 5G, radio over fiber, electronic warfare systems, radar and remote antennas [7-9]. The most spread architecture of MWP systems uses Mach-Zehnder interferometric modulator (MZM) to intensity modulate (IM) the optic carrier and direct detection (DD) to recover the electric signal, commonly referred as MZM IM-DD analog optical link [2].

Just like any other RF system, the main figures of merit to evaluate an MWP system are the power gain (G), the noise figure (NF) and the spurious free dynamic range (SFDR). On MZM IM-DD systems, the gain and the NF are strongly dependent of the incident photodetector optic power (POP). The higher the POP, the higher the gain. But, unfortunately, the photodetector output noise power increases as the POP grows up. Also, in order to avoid harmonic distortion, the MZM is commonly biased at the quadrature point of its electrooptic transfer function, where the second-order harmonics are completely suppressed [2].

The MZM IM-DD link gain depends on the squared optic power and there is no theoretical superior limit to it. However, in practice, it is limited by the photodetector optic saturation power, limited on few milliwatts for high speed commercial devices. On quadrature biased MZM photonic links, the optic carrier to sideband ratio (CSR) is high [8], approximately 20 dB for low signal condition. So, most of the power relies on the optical carrier, which brings the photodetector to the saturation region with no significant contribution to recover the RF signal, since it results from the beating between the carrier and the optic sidebands [5].

To improve the RF recovering efficiency at the photodetector, the CSR reduction is mandatory. Some approaches use nonlinear optic effects to transfer power from the carrier to the sideband, such as four-wave-mixing [7] and parametric amplification of the sidebands [9]. Other approaches move the MZM bias away from the quadrature point to get the carrier power down, known as low biasing technique [5][6][10]. Those approaches have shown good improvement on the system gain, NF and SFDR, comparing to quadrature biased MZM links. As consequence, the system is limited to a sub-octave bandwidth because of the increase on the harmonic distortion. Previous works mentioned above explore those techniques focused on the system performance, not considering the photodetector optic power as a reference

variable. This work investigates the low biasing technique to obtain gain improvement, considering the POP as a constant parameter, compared with the quadrature condition.

Section 2 shows the analytical analysis of the system. Section 3 shows simulations using the expressions deduced in the previous section, with some approximations and considerations. In section 4, experimental results are presented as a proof of concept. Conclusions are presented in section 5.

2 | THEORETICAL FOUNDATION

The schematic diagram of an MZM IM-DD photonic link is shown on Fig. 1. It is composed basically by a laser as the optical source feeding a Mach-Zehnder intensity modulator, followed by a photodetector connected to the MZM by a single-mode optical fiber. To get a general formulation, it is considered a dual drive configuration (DD-MZM), where two independent RF signal are injected into the modulator together with a DC bias voltage to stablish the operation point at the modulator electrooptic transfer function.

It is assumed the lightwave electric field can be expressed by:

$$\vec{\boldsymbol{e}}(t) = Re[E_o e^{j[\omega_o t+\phi_o]}\vec{e}], \tag{1}$$

where E_o is the electrical field amplitude, ω_o is the optic angular frequency, ϕ_o is the initial phase and $\vec{e}$ is the electric field polarization vector. For a sake of clarity, it will be assumed the field polarization does not change through the optic system and can be neglect on the formulation, which will consider only phasor representation from now on and will be referred as optic signal.

The intensity modulation process at the DD-MZM will produce at the output an optic spectrum composed by an optic carrier surrounded by a series of sidebands spaced by multiples of the RF modulating frequency. Neglecting all the losses in the modulator and in the fiber optic path, it can be expressed by [3]:

$$E_m(t) = \frac{E_o}{2} e^{j[\phi_o+\phi_b+\phi_{ps}]\cdot} \sum_{n=-\infty}^{n=+\infty} J_n(m)\cos\left(\phi_{pd}+n\phi_{md}\right) e^{i[(\omega_o+n\omega_m)t+n\phi_{ms}]} \tag{2}$$

where ϕ_b is the absolute phase shift accumulated through the system, $\phi_{ps}=\pi(V_{dc1}+V_{dc2})/2V_\pi$ is the common phase produce by the bias voltages V_{dc1} and V_{dc2} applied to the MZM arms 1 and 2, respectively, V_π is the half wave voltage of the MZM, $J_n(m)$ represents the coefficients of the Bessel functions of first kind of order n, $m = \pi V_m/V_\pi$ is the RF modulation index, $\mathcal{V}_m$ is the modulating signal amplitude, $\phi_{pd}=\pi(V_{dc1}-V_{dc2})/2V_\pi$ is phase difference between the MZM arms produced bias voltages, $\phi_{md}=(\phi_{m1}-\phi_{m2})/2$ and $\phi_{ms}=(\phi_{m1}+\phi_{m2})/2$ are optic phases produced by the two RF modulating signals, where ϕ_{m1} and ϕ_{m2} are its initial phases respectively and ω_m is its angular frequency.

The total power of the spectrum represented by (2) is the sum of the individual powers of each optic component [1]. The optic power at the photodetector, $\mathcal{P}_{d}$, can be expressed by:

$$P_d = P_L K_{po} \sum_{n=-\infty}^{n=+\infty} \left[J_n(m).\cos(\phi_{pd} + n\phi_{md})\right]^2, \tag{3}$$

where P_L is the laser optic power and K_{po} is the link coefficient loss, including the insertion loss of the DD-MZM.

The instantaneous envelope power of the modulated signal is proportional to the product of (2) by its complex conjugated and it is related to its optic intensity [3]. It can be understood as the average power within one period of the carrier lightwave. The RF signal at the photodetector output is proportional to this envelope power [2]. From (2), the photodetector envelope power, $\mathcal{P}_{d}$, can be expressed by:

$$\begin{aligned} P_d(t) = P_L K_{po} \Bigg\{ & \frac{1}{2} \sum_{p=-\infty}^{p=+\infty} J_p{}^2(m)\left[\cos(2\phi_{pd} + 2p\phi_{md}) + 1\right] \\ & + \frac{1}{2} \sum_{k=1}^{k=+\infty} \sum_{p=-\infty}^{p=+\infty} J_p(m) J_{p-k}(m) \Big[\cos(2\phi_{pd} + 2p\phi_{md} \\ & - k\phi_{md})\, e^{i(k\omega_m t + k\phi_{ms})} \\ & + (-1)^k \cos(2\phi_{pd} - 2p\phi_{md} + k\phi_{md}) e^{-i(k\omega_m t + k\phi_{ms})}\Big] \\ & + \frac{1}{2} \sum_{k=1}^{k=+\infty} \sum_{p=-\infty}^{p=+\infty} J_p(m) J_{p-k\,(m)} \cos(k\phi_{md}) \Big[e^{i(k\omega_m t + k\phi_{ms})} \\ & + (-1)^k e^{-i(k\omega_m t + k\phi_{ms})}\Big] \Bigg\} \end{aligned} \tag{4}$$

where *p* represents the orders of the optical spectrum components, and *k* the orders of the RF spectrum components, in other words, the electric harmonics frequencies.

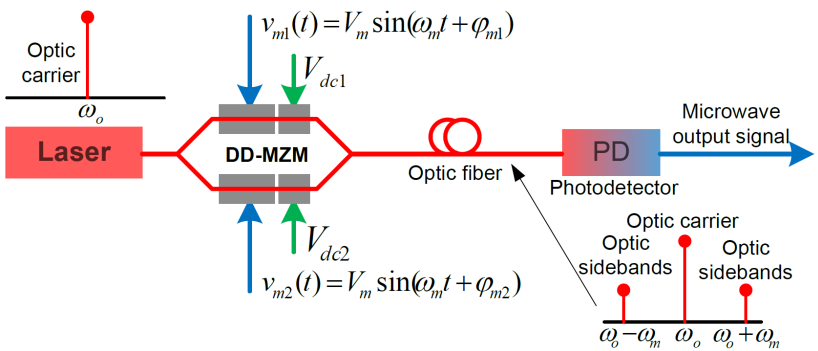

Fig.1 - Microwave photonic link with a DD-MZM configuration and direct detection.

The small signal RF power gain can be calculated taking the fundamental harmonic frequency for $m << 1$. Considering the input and output impedances matched, it can be expressed by [4]:

$$G = \frac{1}{4} K_{po}{}^2 \eta_d{}^2 \left[\frac{\pi P_L}{V_\pi} cos\left(\frac{\pi \Delta V_{dc}}{V_\pi}\right)\right]^2 Z_m Z_L \quad (5)$$

where η_d is the photodetector responsivity, ΔV_{dc} is the DD-MZM voltage bias drift far from the quadrature bias point, expressed by $\Delta V_{dc} = [(V_{dc1} - V_{dc2}) - V_\pi/2]$, Z_m is the DD-MZM input impedance and Z_L is the load output impedance.

3 | SIMULATIONS

It was considered the DD-MZM in a push-pull operation, where $V_{dc1} = -V_{dc2}$ and the phase difference between ϕ_{m1} and ϕ_{m2} is π. The DD-MZM V_π adopted for the simulations is 3.5 V. For simulation, the phases ϕ_o and ϕ_b were considered equal to 0 to simplify (2) and (4).

It was considered V_m = 0.25 V to keep the modulation index on small signal condition, resulting in m = 0.224.

a. Bias voltage at the quadrature point

Based on the previous considerations, the electric field amplitude spectrum from (2) is expressed by:

$$E_m(n) = \frac{E_o}{2}\left[J_n(m)\cos\left(\frac{\pi}{4} + n\frac{\pi}{2}\right)\right] \quad (6)$$

which has the shape shown in Fig. 2, per unit of electric field.

Using (4) to plot Fig. 3, it is possible to realize that the second harmonic does not appear on the expected RF amplitude spectrum.

Appling the quadrature condition in (3) results in:

$$P_d = P_L \sum_{n=-\infty}^{n=+\infty} \left[J_n(m)\cos\left(\frac{\pi}{4} + n\frac{\pi}{2}\right)\right]^2 \quad (7)$$

which reveals that, together (6), it is possible to decrease the carrier, n=0, and increase the sidebands, n= ±1, by growing up the cosine bias argument ϕ_{pd}, toward to $\pi/2$. Fig. 4 shows that condition. Equation (2) and the red lines in Fig.4 reveal that there is a high CSR penalty to eliminate the second-order harmonics,

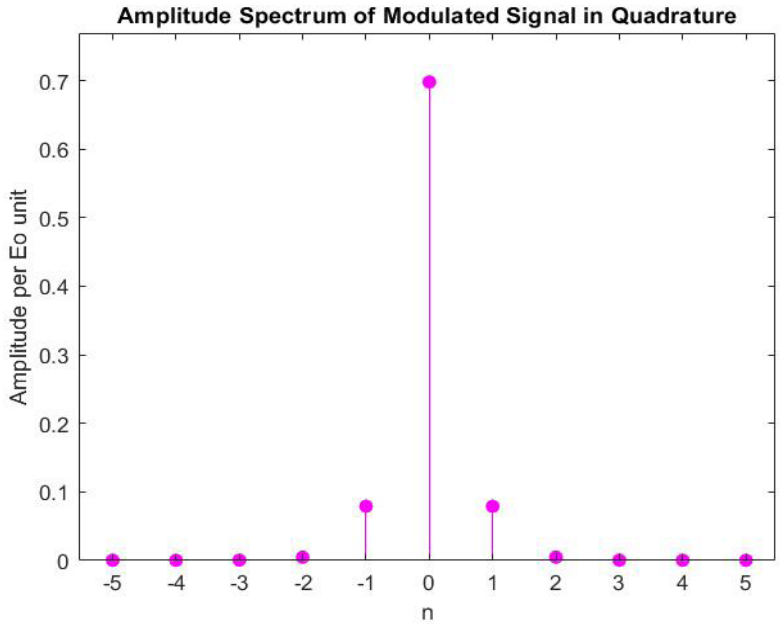

Fig.2 - Optic amplitude spectrum of the modulated signal, at quadrature bias condition and m=0.244.

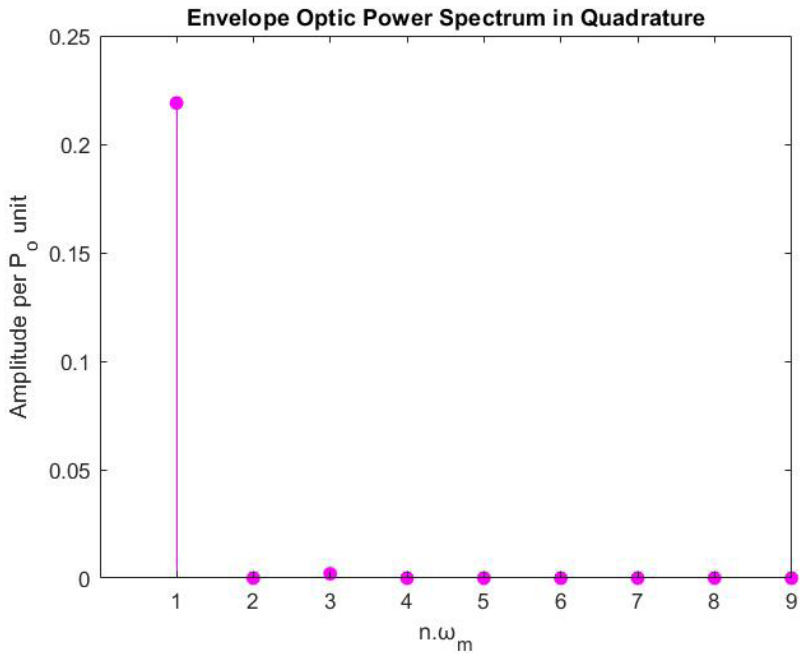

Fig.3 - Optic power envelope spectrum per unit of P_L, at quadrature bias condition and K_{po} unitary.

i.e, the cosine amplitude factor in (6) and (7) is the same for the carrier and sidebands components. For low modulation indexes, the carrier power is much bigger than the

sidebands and does not contribute to recover the RF output signal efficiently. This effect goes down with the modulation index increasing, but it keeps still high for practical condition. Consequently, increasing the laser power will bring the photodetector to saturation without produce link RF power gain efficiently.

b. Shifting bias voltage far from the quadrature point

By inspection of (2) and starting from the quadrature condition, the best bias voltage to optimize the beating between the carrier and the sidebands can be calculated for a given modulation index. The best beating efficiency will occur when the amplitude of the two components are equals. From (2) this bias condition can be determined, resulting in:

$$\phi_{pd\_opm} = \tan^{-1}\left(\frac{J_0(m)}{J_1(m)}\right). \tag{8}$$

For the same modulation condition adopted for the quadrature case, m = 0.224, ϕ_{pd_opm} is 1.46 and the amplitude spectrum of (2) becomes:

$$E_m(n) = \frac{E_o}{2}\left[J_n(m)\cos\left(1.46 + n\frac{\pi}{2}\right)\right] \tag{9}$$

which are shown in Fig. 5.

The blue dotted lines in Fig. 4 also shows, together (9), that the Bessel functions coefficients continues with a great difference between then, but the cosine amplitude factor attenuates the carrier and increases the sidebands, bringing the optics components to the same amplitude to achieve the highest beating efficiency.

The total power incident at the photodetector is calculated from (3), expressed by:

$$P_d = P_L \sum_{n=-\infty}^{n=+\infty}\left[J_n(m).\cos\left(1.46 + n\frac{\pi}{2}\right)\right]^2 \tag{10}$$

The photodetector output RF signal spectrum is shown in Fig. 6, where it can be seeing the presence of the second harmonic.

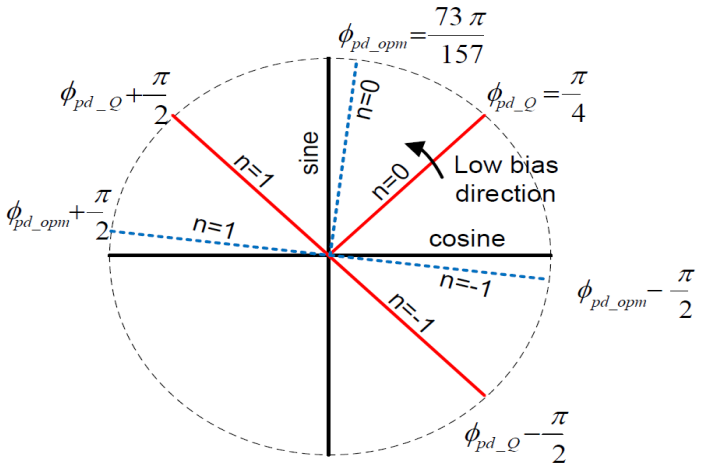

Fig.4 - Trigonometric circumference plotting of the cosine argument ($\phi pd + n\,\pi/2$).

Red lines represent the quadrature condition. Dotted blue lines represent the low bias condition.

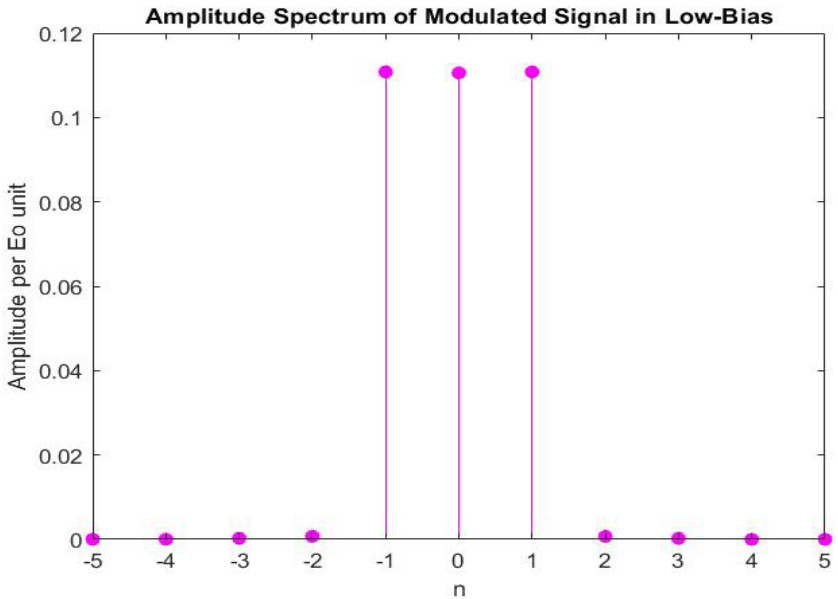

Fig.5 - Optic spectrum amplitude of the modulated signal, at optimum MZM bias condition.

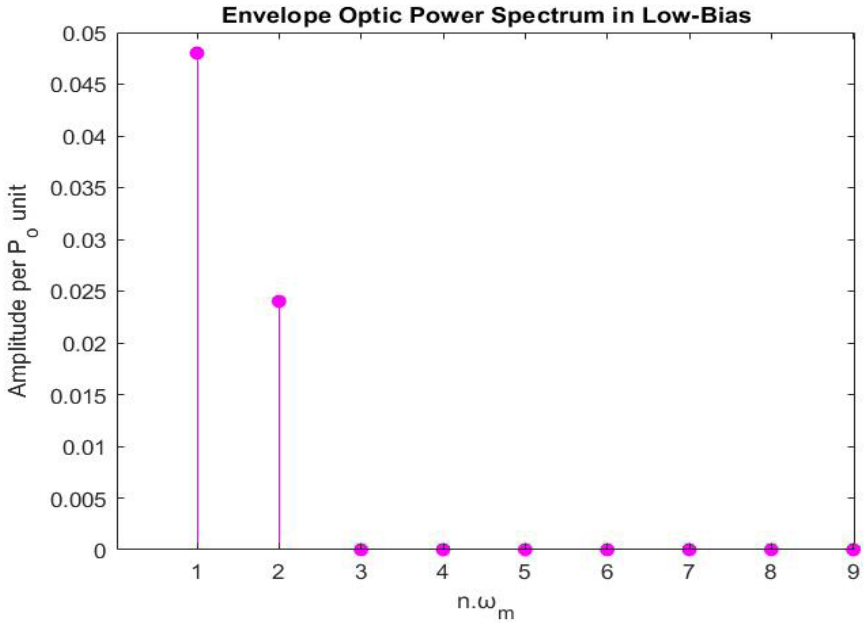

Fig. 6 - Optic power envelope spectrum per unit of P_L and K_{po} unitary, at optimum MZM bias condition.

c. Link RF power gain

Fig. 7 shows a comparative plot of the RF power gain of the link, considering the two conditions assumed above and equation 5. It was considered $Z_m = Z_L = 50\Omega$, and k_{po} and η_d unitary. As can be seen in Fig. 7, the gain for optimal bias condition is 9.7 dB above the gain in quadrature, for the same incident optic power at the photodetector.

4 | EXPERIMENT

Fig. 8 shows the schematic diagram of the experiment setup. Similarly to simulations, the experiment was carried out with the MZM operating upon a push-pull configuration. The optic carrier is from a DFB laser, tuneded at the wavelengh of 1552.54 nm, with a maximal power of 100 mW when drived by a current of 454.72 mA.

A laser drive controls the temperature and the current in the DFB laser. The optical carrier is coupled into a Mach-Zehnder intensity modulator with 10.

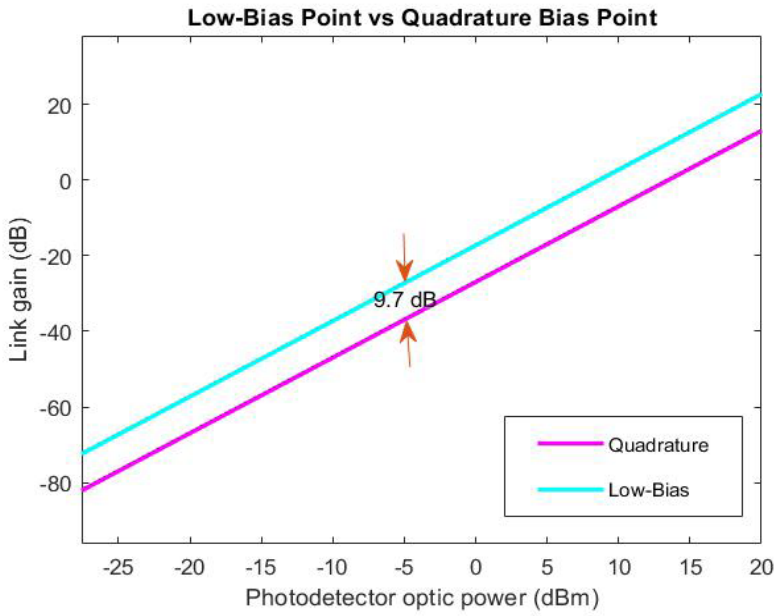

Fig.7 - Comparative plot of the RF link power gain. Quadrature condition in purple line and low bias condition in blue line.

GHz of bandwidth, from EOspace Inc, with a mesured insertion loss of 5 dB, a RF V_π of 6.54 V, a bias V_π of 6.3 V and input impedance of 50 . A symetric DC power supply of +/-10 V feeding a potenciometer was used to regulate the bias voltage into the MZM, measured by a digital voltimetre. An RF signal generator feeds the MZM with the modulating signal.

To measure the optical spectrum, it was inserted before the photodetector a 90/10 fiber coupler, taking 10% of the modulated optic signal to an optical spectrum analyzer (OSA) and injecting 90% into a high speed photodiode, from New Focus Inc, with responsivity of 0.6 A/W, saturation power of 8 mW, output impedance of 50 Ω and bandwidth of 25 GHz. A multimeter was used to measure the incident power on photodiode, using a low frequency transimpedance amplifier available in the photodetector module, with 1 kΩ of gain. The RF photodetector output signal is injected into an RF amplifier, from Miteq Inc, to feed an electric spectrum analyzer (ESA). The RF power gain of the amplifier is 40 dB at 7 GHz, with an input and output impedances of 50 Ω, powered by a DC power supply of 15 V. The fiber path is a single mode fiber and the total losses are 3.3 dB.

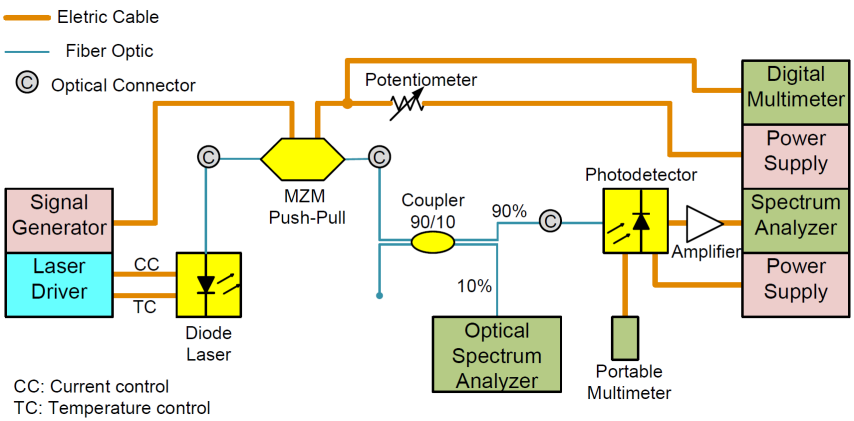

Fig.8 - Schematic diagram of the experiment setup.

To achieve an RF signal amplitude of 0.25 V, the same value used for the simulations, the signal generator power was adjusted to 3.44 dBm at a frequency of 7 GHz. The first gain measurement was taken for the low bias condition. Measuring the optic signal on the OSA, the MZM bias voltage was adjusted to get a CSR of 0 dB as shown in Fig. 9 (left).

So, the laser power was set to its maximum, P_L = 100 mW. The transimpedance amplifier output marked 48 mV at this point. The fundamental RF frequency output signal measure was -12.98 dBm, as shown in Fig. 9 (right). Taking out the RF amplifier gain, the intrinsic link gain was -52.98 dB.

Then, the MZM bias voltage was adjusted to the quadrature point, where the second harmonic is canceled. The laser power was decreased to obtain the same value at the photodetector for the low bias condition, that is, 48 mV at the transimpedance output. On that condition, the laser power was 2.57 mW. The optic spectrum was measured, and it is shown in Fig. 10 (left), with a measured CSR of 16.12 dB.

The fundamental RF output signal is -20.61 dBm, and its spectrum is shown in Fig. 10 (right), with no second harmonic observed. The intrinsic link gain is -60.61 dB, that is, 7.63 dB below the low bias condition gain. Due to the MZM electrooptic transfer function instability and the absence of an automatic bias control circuit, there was an uncertainty on the measurements and was considered as about 2 dB, after several sequential observations.

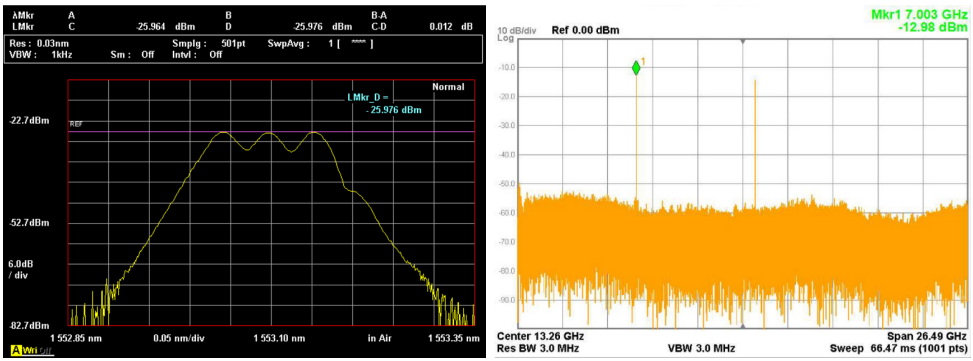

Fig.9 – Left: optic modulated signal spectrum at low bias condition. Right: RF output signal spectrum at low bias condition.

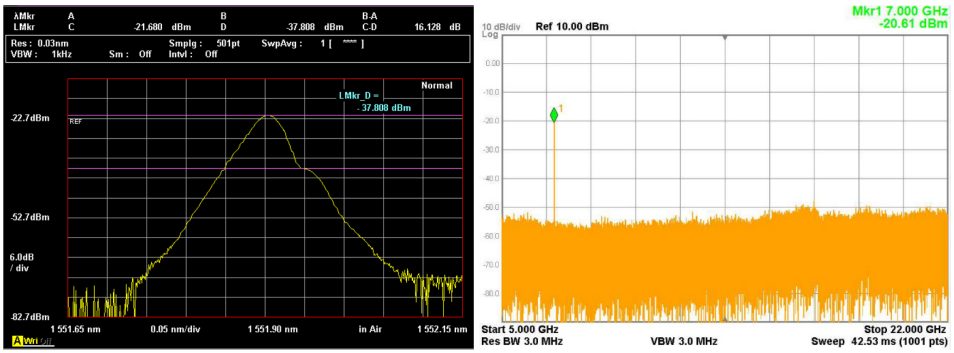

Fig. 10 – Left: Optic modulated signal spectrum at quadrature bias condition. Right: RF signal output spectrum at quadrature bias condition.

5 I CONCLUSION

The beating of the optic spectral components at the photodetector was investigated to optimize the power efficiency to recover the RF signal at the sub-octave link output, considering the photodetector saturation power as the bottleneck of the system. It was demonstrated the best condition is when the CSR is 0 dB, and there is a RF link power gain improvement of 9.7 dB for the same photodetector optic power.

AKNOWLEDGMENT

This work was supported by the Brazilian Air Force at the Electronic Warfare Laboratory of ITA, by the Ecole Nationale d'Ingénieurs de Brest (ENIB) - France, and by the Coordenação de Aperfeiçoamento de Pessoal de Nível Superior – Brasil (CAPES).

REFERÊNCIAS

CARVALHO, R. M. **Princípios de comunicações**. Vitoria: [s.n.], 2000.

CHANG, W. S. C. **RF photonic technology in optical fiber links**. New York: Cambridge University Press, 2002.

CORRAL, J. L.; MARTI, J.; FUSTER, J. M. General expressions for IM/DD dispersive link analog optical links with external modulation or optical up-conversion in a Mach-Zehnder eletrooptical modulator. **IEEE Trans Microw Theory Tech,** New York, v. 49, n. 10, Oct. 2001.

COUTINHO, O. L.; ALMEIDA, V. R.; OLIVEIRA, J. E. B. Uso de redes de comunicações ópticas para transmissão e distribuição de emissores radar. *In:* Simpósio de Aplicações Operacionais em Áreas de Defesa, 8., São José dos Campos, Set. 2011. **Anais** [...]. São José dos Campos: Instituto Tecnológico de Aeronáutica, [2011?].

DEVENPORT, J.; KARIM, A. Optimization of an externally modulated RF photonic link. **Fiber and Integrated Optics**, Carlsbad, v. 27, p. 7-14, Dec. 2007.

FARWELL, M. L.; CHANG, W. S. C.; HUBER, D. R. Increased linear dynamic range by low biasing the Mach-Zehnder modulator. **IEEE Photonics Technol Lett**, New York, v. 5, n. 7, July 1993.

FILGUEIRAS, H. R. D.; BRANDÃO, T. H.; BORGES, R. M.; CERQUEIRA Jr., A. S. New topology and digital performance analysis of a photonics-based RF amplifier. *In*: Simpósio Brasileiro de Micro-ondas e Optoeletrônica, 18., Congresso Brasileiro de Eletromagnetismo,13., 2018, Santa Rita do Sapucaí. **Anais** [...]. São Caetano do Sul: Simpósio Brasileiro de Micro-ondas e Optoeletrônica, p. 644-648, 2018.

GAO, Y.; WEN, A.; PENG, Z.; TU, Z. Analog photonic link with tunable optical carrier to sideband ratio and balanced detection. **IEEE Photonics J**, Piscataway, v. 9, n. 2, Apr. 2017.

MARQUES, R. B.; CASTRO, J. J. B.; OLIVEIRA, J. E. B. Modelagem e demonstração da amplificação paramétrica de sinais de RF em enlace analógico a fibra óptica. *In*: Simpósio Brasileiro de Micro-ondas e Optoeletrônica, 18., Congresso Brasileiro de Eletromagnetismo,13., 2018, Santa Rita do Sapucaí. **Anais** [...]. São Caetano do Sul: Simpósio Brasileiro de Micro-ondas e Optoeletrônica, p. 644-648, 2018.

URICK, V. J.; GODINEZ, M. E.; DEVGAN, P. S.; MCKINNEY, J. D.; BUCHOLTZ, F. Analysis of an analog fiber-optic link employing a low-biased Mach-Zehnder modulator followed by an erbium-doped fiber amplifier. **J Lightwave Technol**, New York, v. 27, n. 12, June 15, 2009.

ÍNDICE REMISSIVO

V

COLEÇÃO

DESAFIOS DAS ENGENHARIAS:

ENGENHARIA ELÉTRICA 2

www.atenaeditora.com.br
contato@atenaeditora.com.br
@atenaeditora
www.facebook.com/atenaeditora.com.br

Atena Editora
Ano 2021

COLEÇÃO

DESAFIOS DAS ENGENHARIAS:

ENGENHARIA ELÉTRICA 2

www.atenaeditora.com.br
contato@atenaeditora.com.br
@atenaeditora
www.facebook.com/atenaeditora.com.br

Atena Editora
Ano 2021